On the redundant and non-redundant virtual turning points for the AKT equation (Several aspects of microlocal analysis)

AUTHOR(S):

Hirose, Sampei

CITATION:

Hirose, Sampei. On the redundant and non-redundant virtual turning points for the AKT equation (Several aspects of microlocal analysis). 数理解析研究所講究録別冊 2016, B57: 39-59

ISSUE DATE:

2016-05

URL:

http://hdl.handle.net/2433/241331

RIMS Kôkyûroku Bessatsu
B57 (2016), 039–059

On the redundant and non-redundant virtual turning points for the AKT equation

By

Sampei HIROSE*

Abstract

In this note we study how the Stokes geometry of the AKT equation, which is obtained by restricting the (1,4) hypergeometric system of two variables (x_1, x_2) onto $x_2 = c$, changes when the parameter c changes. In particular, we show with the help of a computer that some redundant virtual turning point of the AKT equation becomes a non-redundant one when c changes.

§ 1. Introduction

In our previous paper [2], we investigate the relationship between the Stokes geometry of the (1,4) hypergeometric system

$$\begin{cases} \left(\eta^{-3}\dfrac{\partial^3}{\partial x_1^3} + \dfrac{2}{3}x_2\eta^{-2}\dfrac{\partial^2}{\partial x_1^2} + \dfrac{1}{3}x_1\eta^{-1}\dfrac{\partial}{\partial x_1} - \dfrac{\alpha}{3}\right)\psi = 0, \\ \left(\eta^{-1}\dfrac{\partial}{\partial x_2} - \eta^{-2}\dfrac{\partial^2}{\partial x_1^2}\right)\psi = 0 \end{cases}$$

and that of the AKT equation (or AKT_c equation)

$$\left(\eta^{-3}\frac{d^3}{dx_1^3} + \frac{2}{3}c\eta^{-2}\frac{d^2}{dx_1^2} + \frac{1}{3}x_1\eta^{-1}\frac{d}{dx_1} - \frac{\alpha}{3}\right)\psi = 0,$$

which is obtained by restricting the (1,4) hypergeometric system to $x_2 = c$. In this paper, based on this work [2], we study how the Stokes geometry (ordinary and new Stokes curves, ordinary and virtual turning points) of the AKT_c equation changes when

Received February 1, 2016. Revised February 9, 2016. Accepted February 9, 2016.
2010 Mathematics Subject Classification(s): 34E20, 34M60
Key Words: *virtual turning point, new Stokes curve, AKT equation.*
Supported by JSPS KAKENHI Grant No.15K17556.
*Center for Promotion of Educational Innovation, Shibaura Institute of Technology, 307 Fukasaku, Minuma-ku, Saitama-shi, Saitama 337-8570, Japan.

the parameter c changes. Our emphasis in this paper is put on clarifying the global effect of virtual turning points that appear in the Stokes geometry in question; to be more precise, we confirm with the help of a computer that some redundant virtual turning point of the AKT_c equation turns out to be a non-redundant one in the $\mathrm{AKT}_{c'}$ equation for a point c' that is sufficiently close to c. Furthermore we confirm in the example we study below that such a change is observed along a curvilinear half line (§3). This novel intriguing result is an important starting point of our future study how to introduce a proper definition of the redundancy of virtual turning points in an equation depending on parameters (such as the AKT_c equation).

The author would like to express his thanks to Professor Takahiro Kawai and Professor Yoshitsugu Takei for their many valuable advices and encouragements.

§ 2. Review of the Stokes geometry for the AKT equation

In this section we recall some basic facts concerning the Stokes geometry of the AKT equation. They are obtained in [2] in conjunction with the study of the (1,4) hypergeometric system, and we refer the reader to [2] for the details. To help the understanding of the reader, we put the order relations (such as $1 < 2, 2 < 1$ etc.) to some Stokes curves which play important roles in our study in §3.

First, the ordinary turning points of the AKT_c equation are, by definition, given by the following

$$12x_1^3 - 4c^2x_1^2 + 108\alpha c x_1 + 243\alpha^2 - 32\alpha c^3 = 0. \tag{2.1}$$

Figure 1 shows the configuration of ordinary turning points of the AKT_c equation and Stokes curves emanating from them for $c = \sqrt{-1}/20, \alpha = 1/2 - \sqrt{-1}/2$. Following the Ansatz given in [1] and adding new Stokes curves emanating from non-redundant virtual turning points to Figure 1, we obtain Figure 2. Note that, as explained in [4],

- A new Stokes curve is inert until it hits an ordered crossing point.
- If a new Stokes curve hits an ordered crossing point, its portion after passing over the crossing point becomes active.
- A virtual turning point is said to be redundant if a new Stokes curve emanating from it never hits an ordered crossing point. A virtual turning point which is not redundant is called non-redundant.

(In Figure 2, we do not distinguish active portions and inert portions for new Stokes curves; all new Stokes curves are drawn by solid line there.) In the case of the AKT equation, as was confirmed in [2] with the aid of a computer, the number of new Stokes

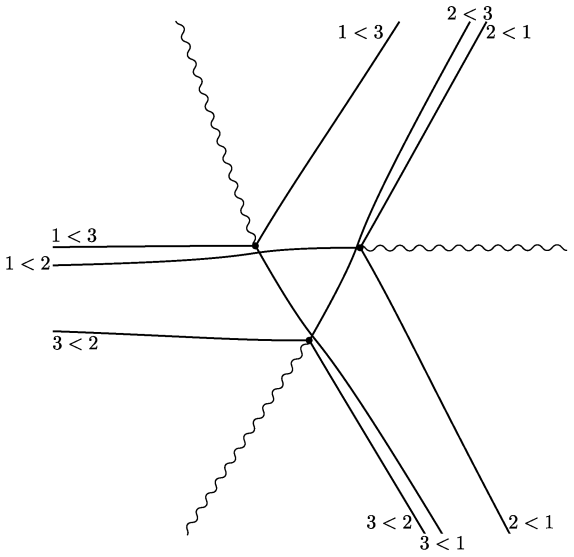

Figure 1. The ordinary turning points and the ordinary Stokes curves of the AKT_c equation for $c = \sqrt{-1}/20, \alpha = 1/2 - \sqrt{-1}/2$.

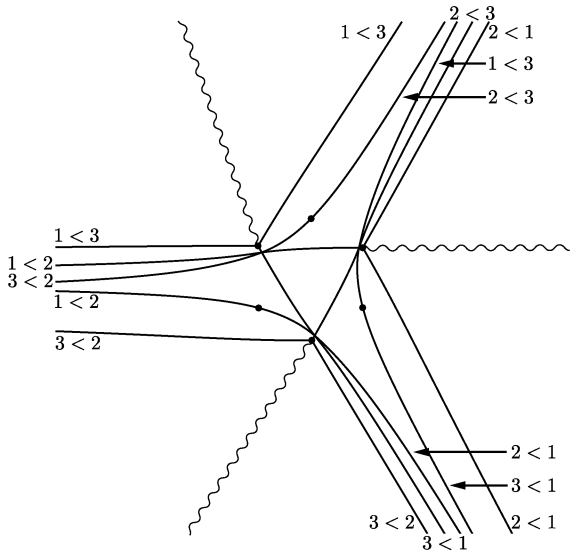

Figure 2. Figure 1 with new Stokes curves emanating from non-redundant virtual turning points being added.

curves emanating from non-redundant virtual turning points is finite although it has infinitely many virtual turning points.

Let $c_j^{(0)}$ $(j = 1, 2, 3)$ be a zero of the discriminant of (2.1) for the variable x_1, which is explicitly given by

$$c_j^{(0)} = -\frac{3^{5/3}}{2}\alpha^{1/3}e^{2\pi\sqrt{-1}(j-1)/3} \quad (j = 1, 2, 3).$$

Let H denote the c-plane with cuts emanating from $c_j^{(0)}$ (cf. Figure 3). On H each ordinary turning point of the AKT_c equation is expressed by a single-valued function $a_j(c)$ $(j = 1, 2, 3)$ of c. Without loss of generality, we may assume that

$$a_j(c_j^{(0)}) = a_{j+1}(c_j^{(0)}) \quad (j = 1, 2, 3)$$

and

$$\xi_j\Big|_{(x_1,x_2)=(a_j(0),0)} = \xi_{j+1}\Big|_{(x_1,x_2)=(a_j(0),0)} \quad (j = 1, 2, 3)$$

hold, where ξ_j $(j = 1, 2, 3)$ denotes a root of

$$\xi^3 + \frac{2}{3}x_2\xi^2 + \frac{1}{3}x_1\xi - \frac{\alpha}{3} = 0.$$

Here and in what follows, the indices j of $c_j^{(0)}$, $a_j(c)$ and ξ_j are assumed to be considered by mod 3.

In our study in §3, the curves defined by the following relation play an important role.

(2.2)
$$\Im\left(\int_{a_i(c)}^{a_{i+1}(c)}(\xi_i(x_1,c)-\xi_{i+1}(x_1,c))\,dx_1-2\pi\sqrt{-1}\alpha k\right)=0,$$
$$\Im\left(\int_{a_{i+1}(c)}^{a_i(c)}(\xi_{i+1}(x_1,c)-\xi_{i+2}(x_1,c))\,dx_1-2\pi\sqrt{-1}\alpha k\right)=0\quad(i=1,2,3,k\in\mathbb{Z}).$$

Figure 4, which coincides with Figure 15 in [2], shows the curves for $k=0$. It is observed in [2] that, if c lies on the curves (2.2) for $k=0$, a Stokes curve emanating from an ordinary turning point hits another ordinary turning point, say a. We note also that in this situation a new Stokes curve emanating from a virtual turning point simultaneously hits the same ordinary turning point a; this observation is a starting point of our study in this paper. Similarly, if c lies on the curves (2.2) for $k\neq 0$, two new Stokes curves emanating from virtual turning points hit one ordinary turning point (cf. [2]). Note that the curves (2.2) can be thought of as curves emanating from zeros of the following function

(2.3)
$$\int_{a_i(c)}^{a_{i+1}(c)}(\xi_i(x_1,c)-\xi_{i+1}(x_1,c))\,dx_1-2\pi\sqrt{-1}\alpha k,$$
$$\int_{a_{i+1}(c)}^{a_i(c)}(\xi_{i+1}(x_1,c)-\xi_{i+2}(x_1,c))\,dx_1-2\pi\sqrt{-1}\alpha k\quad(i=1,2,3,\ k\in\mathbb{Z}).$$

Figure 5 shows the curves (2.2) for $k=0,\pm1,\dots,\pm6$ and, by adding zeros of (2.3) for $k=0,\pm1,\dots,\pm6$ to Figure 5, we obtain Figure 6. It is also observed in [2] that an ordinary turning point merges with another ordinary turning point at a zero of (2.3) for $k=0$ and that two virtual turning points merge with an ordinary turning point at a zero of (2.3) for $k\neq 0$. (At a zero of (2.3) for $k=0$ a virtual turning point also merges with the ordinary turning point mentioned above simultaneously.)

§ 3. Redundant and non-redundant virtual turning points for the AKT equation

In [2] we studied how new Stokes curves of the AKT_c equation changes with the parameter c, but we did not study which portion of new Stokes curves is active or inert, or whether a virtual turning point in question is redundant or non-redundant. In this section, we consider the change of the Stokes geometry more carefully, that is, with distinguishing inert portions of new Stokes curves from active ones and redundant virtual turning points from non-redundant ones.

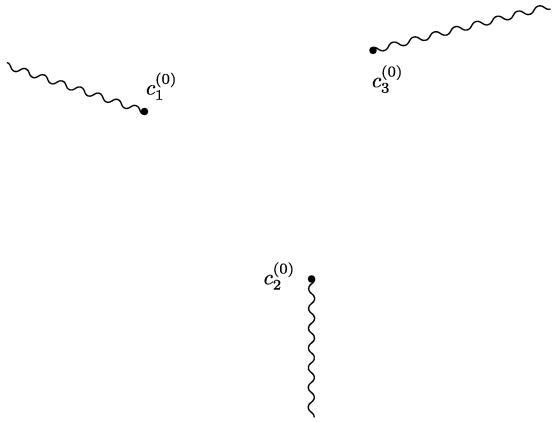

Figure 3. The cut plane H.

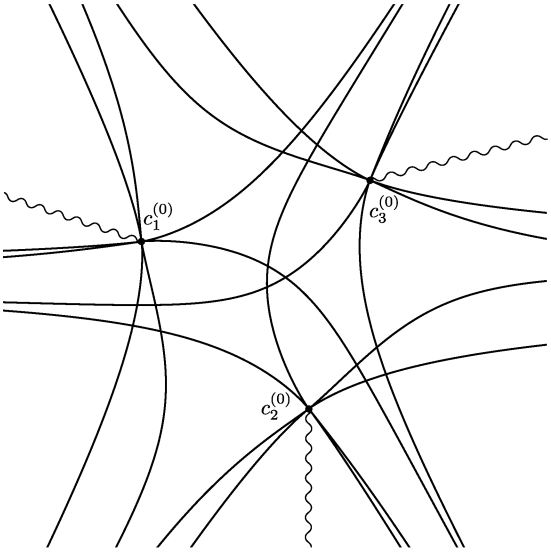

Figure 4. The curves (2.2) for $k = 0$.

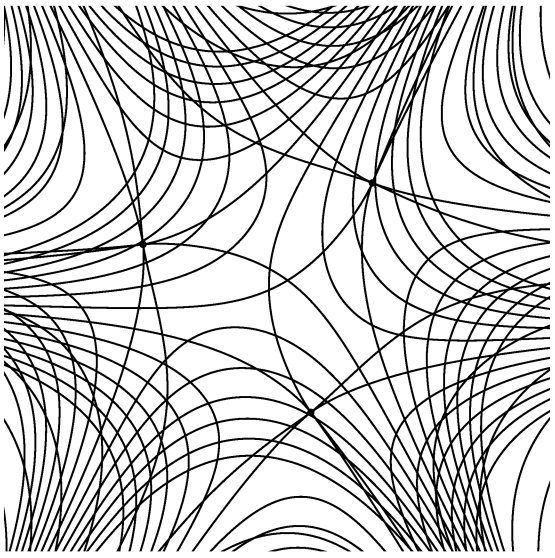

Figure 5. The curves (2.2) for $k = 0, \pm 1, \ldots, \pm 6$.

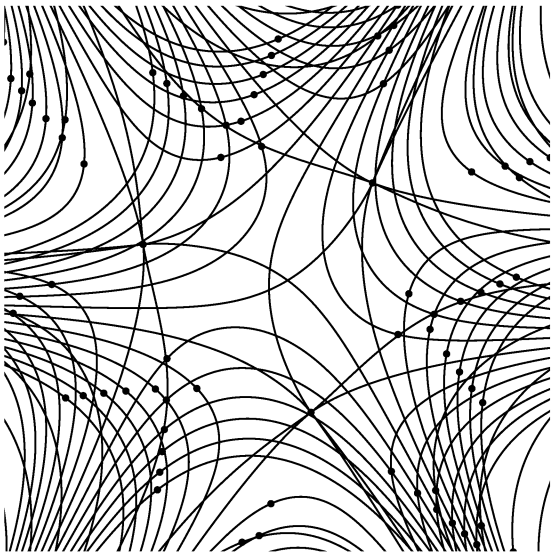

Figure 6. Figure 5 with zeros of (2.3) for $k = 0, \pm 1, \ldots, \pm 6$ being added.

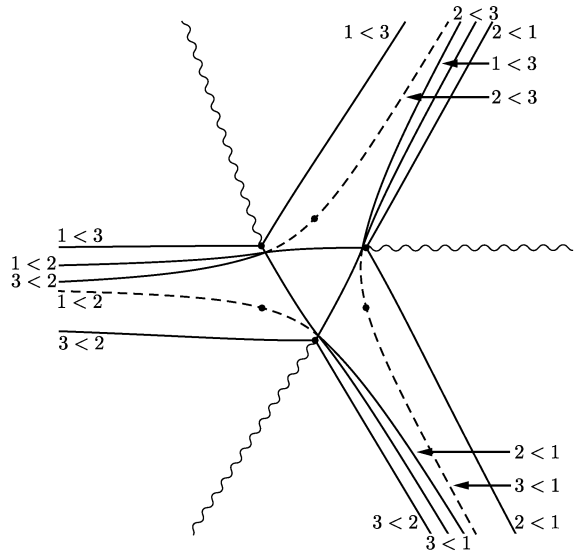

Figure 7. The Stokes geometry shown in Figure 2. Here an inert (resp., active) portion of new Stokes curves is drawn by dotted (resp., solid) line.

First, we present Figure 7 corresponding to Figure 2: In Figure 7 an inert (resp., active) portion of new Stokes curves is drawn by dotted (resp., solid) line. As in Figure 7, we use dotted line to designate an inert portion of new Stokes curves in what follows.

Now let us consider a zero $c^{(k)}$ of

$$\int_{a_3(c)}^{a_1(c)} (\xi_3(x_1,c) - \xi_1(x_1,c))dx_1 - 2\pi\sqrt{-1}\alpha k = 0, \tag{3.1.k}$$

for $k = 1, 2, \ldots$ and a curve

$$\Im\left(\int_{a_3(c)}^{a_1(c)} (\xi_3(x_1,c) - \xi_1(x_1,c))dx_1 - 2\pi\sqrt{-1}\alpha k\right) = 0 \tag{3.2.k}$$

emanating from $c^{(k)}$. Note that the curve (3.2.k) is a part of (2.2). See Figure 8, where $c^{(k)}$ and the curves (3.2.k) for $k = 1, 2$ are added to Figure 4.

We first study the change of Stokes geometry of the AKT_c equation when c moves on a small loop γ encircling $c^{(1)}$. We take points $c_1, \ldots c_{17}, c_{18} = c_1$ on γ as shown in Figure 9. Among them c_2 and c_{10} are situated on the curve (3.2.k) for $k = 1$. Figures $10, \ldots, 27$ show the Stokes geometry of the AKT_c equation for $c = c_1, \ldots, c_{18}$. Figures $28, \ldots, 45$ are their enlarged versions around $a_1(c)$. In these enlarged figures, two virtual turning points are observed; in Figure 28 we label them as v_1, v_2, and use the same labels for their analytic continuations along γ in the other figures. (In these figures, to distinguish new Stokes curves emanating from v_1 and v_2, we designate the

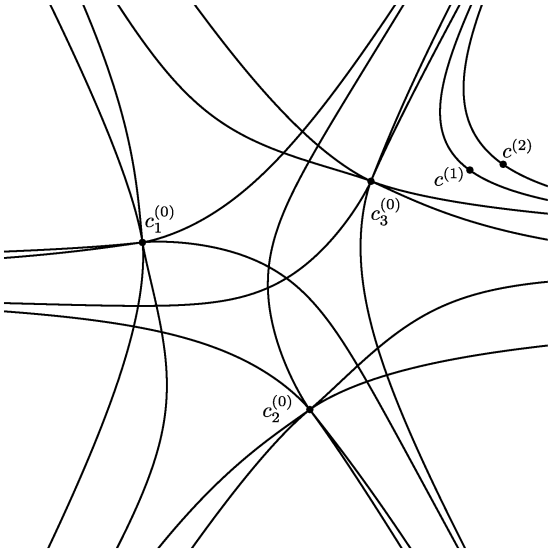

Figure 8. Figure 4 with $c^{(k)}$ and the curves $(3.2.k)$ for $k = 1, 2$ being added.

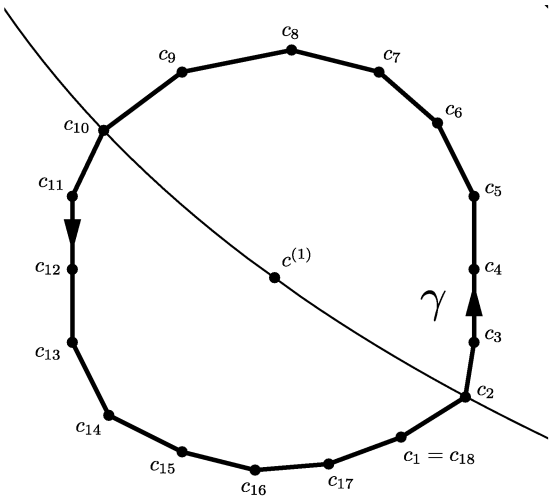

Figure 9. $c^{(1)}$ and c_j $(j = 1, \ldots, 18)$ on γ.

new Stokes curve emanating from v_1 by chain line and that emanating from v_2 by two-dot chain line, respectively.)

We have observed the following facts in [2]:

- The two virtual turning points v_1 and v_2 are interchanged after the analytic continuation along γ.
- At $c = c_2$ and c_{10}, new Stokes curves emanating from v_1 and v_2 hit the ordinary turning point $a_1(c)$.

In view of Figures $10, \ldots, 45$, we now observe the following facts for the redundancy of v_1 and v_2:

- v_1 is non-redundant and v_2 is redundant for $c = c_1, \ldots, c_9$.
- At $c = c_{10}$, the new Stokes curves emanating from v_1 and v_2 simultaneously hit the ordinary turning point $a_1(c_{10})$ and consequently the redundancy of v_1 and v_2 can not be determined.
- v_1 is redundant and v_2 is non-redundant for $c = c_{11}, \ldots, c_{18}$.

That is, at $c = c_{10}$ a redundant virtual turning point is changed to a non-redundant one, whereas such a change does not occur at $c = c_2$.

To visualize these changes more clearly, we let $c_{2-\varepsilon}$ (resp., $c_{2+\varepsilon}$) denote the point just before (resp., shortly after) c reaches c_2 and present the Stokes geometry at these

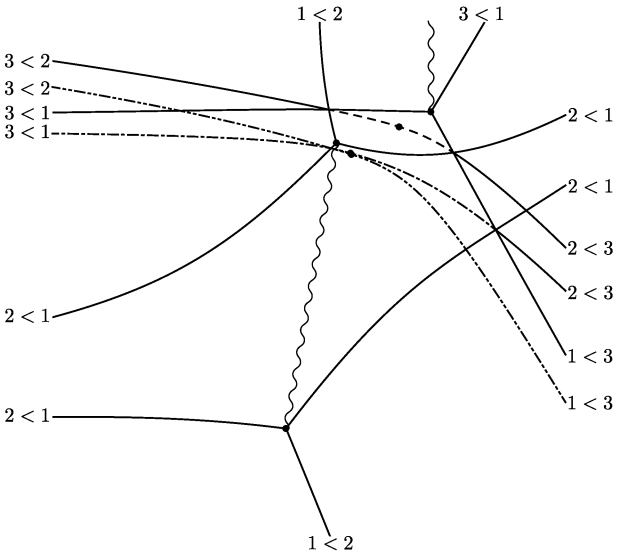

Figure 10. The Stokes geometry of the AKT_c equation for $c = c_1$.

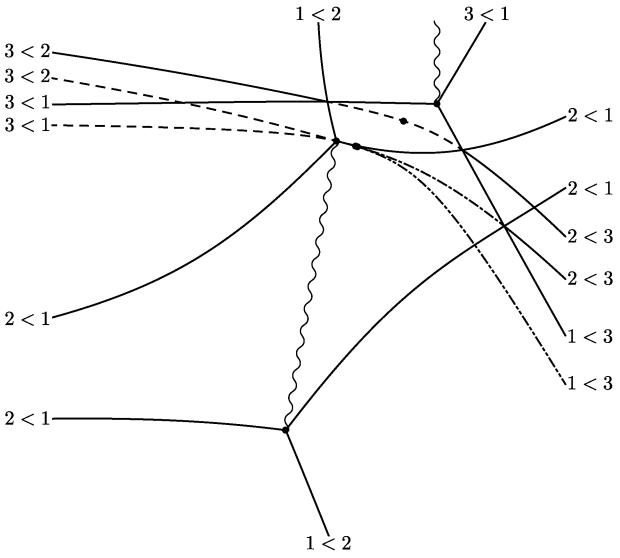

Figure 11. The Stokes geometry of the AKT_c equation for $c = c_2$.

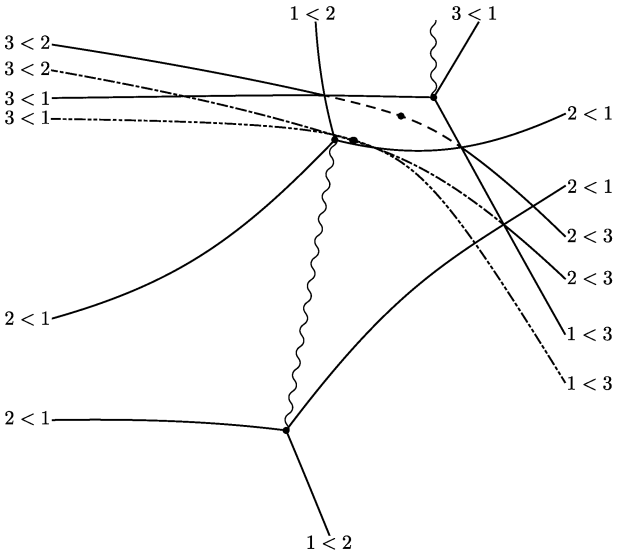

Figure 12. The Stokes geometry of the AKT_c equation for $c = c_3$.

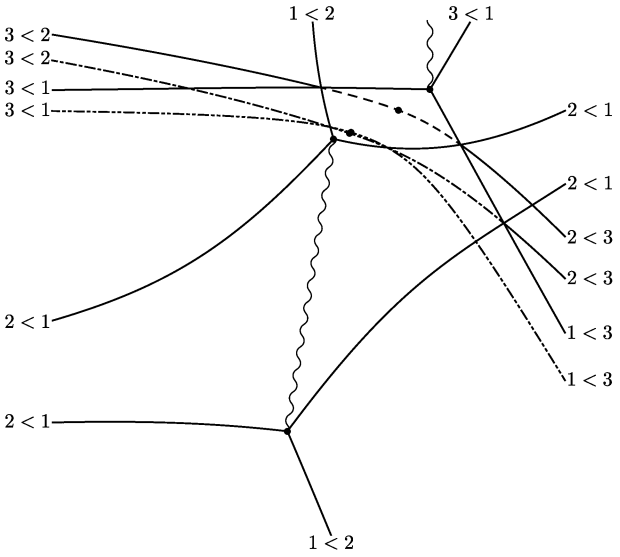

Figure 13. The Stokes geometry of the AKT_c equation for $c = c_4$.

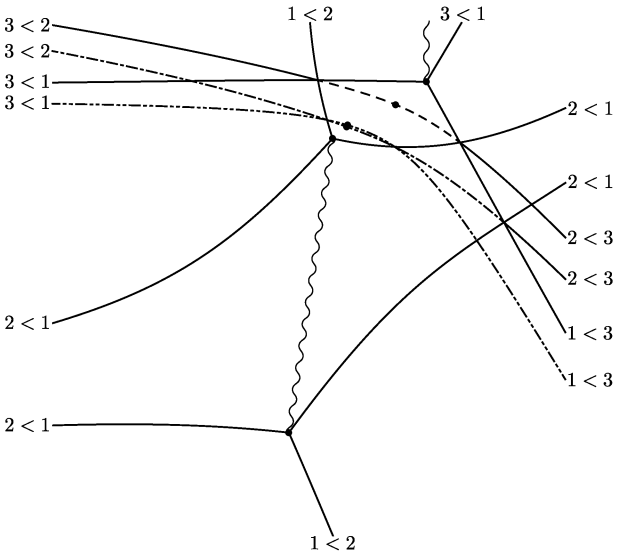

Figure 14. The Stokes geometry of the AKT_c equation for $c = c_5$.

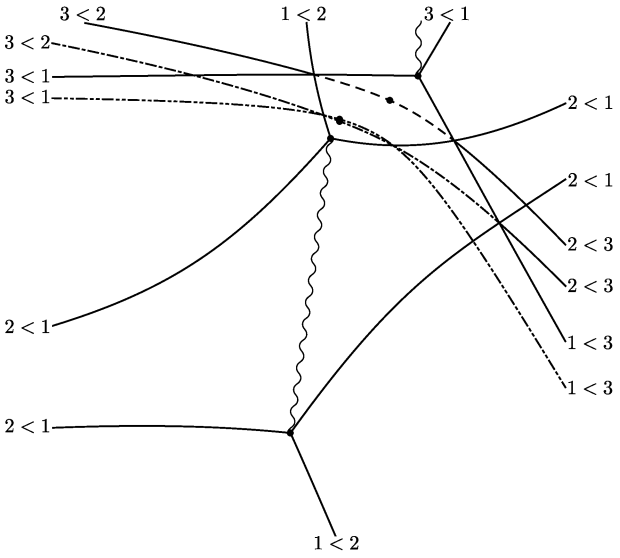

Figure 15. The Stokes geometry of the AKT_c equation for $c = c_6$.

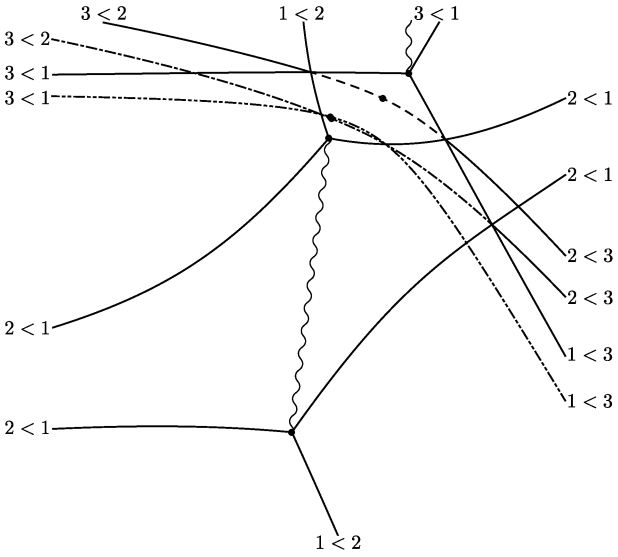

Figure 16. The Stokes geometry of the AKT_c equation for $c = c_7$.

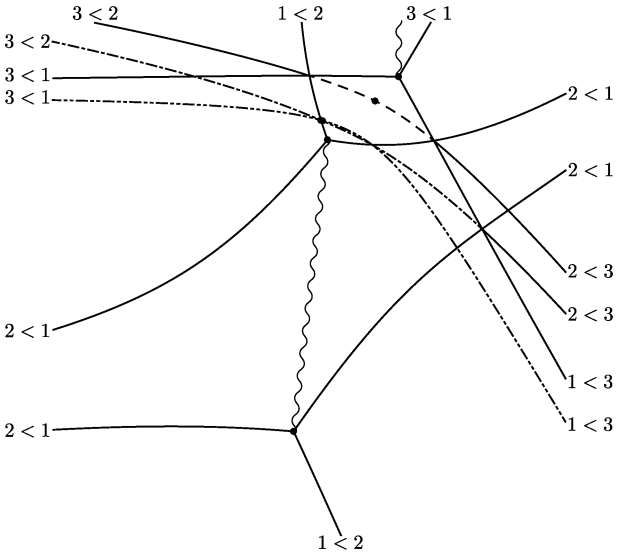

Figure 17. The Stokes geometry of the AKT_c equation for $c = c_8$.

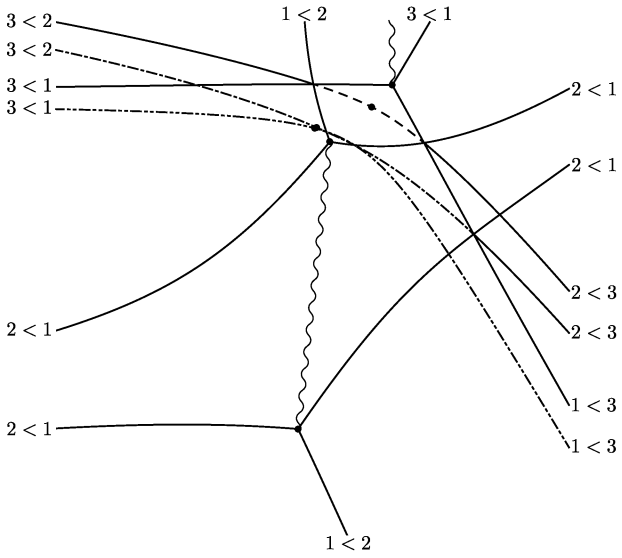

Figure 18. The Stokes geometry of the AKT_c equation for $c = c_9$.

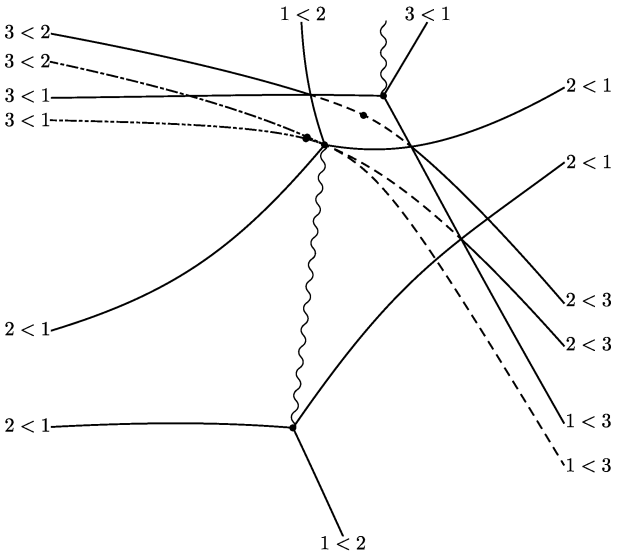

Figure 19. The Stokes geometry of the AKT_c equation for $c = c_{10}$.

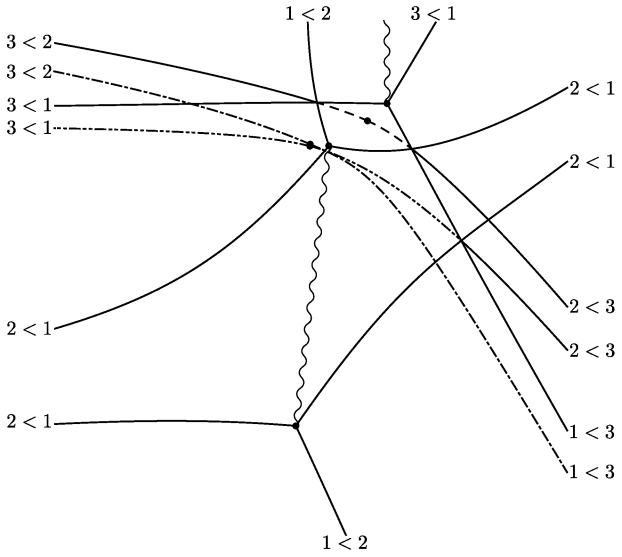

Figure 20. The Stokes geometry of the AKT_c equation for $c = c_{11}$.

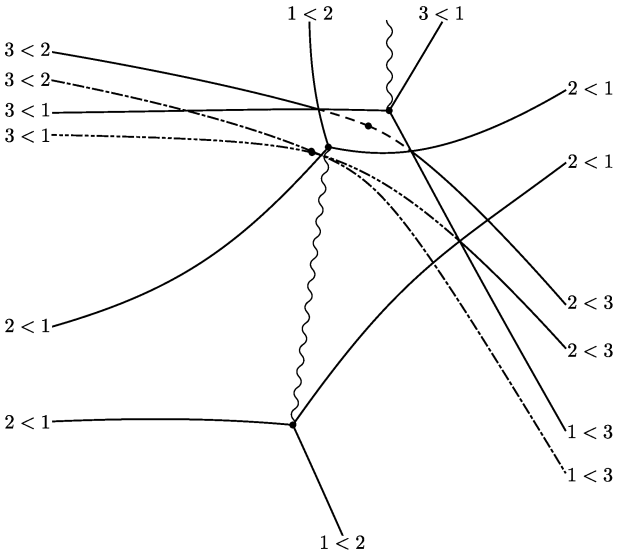

Figure 21. The Stokes geometry of the AKT_c equation for $c = c_{12}$.

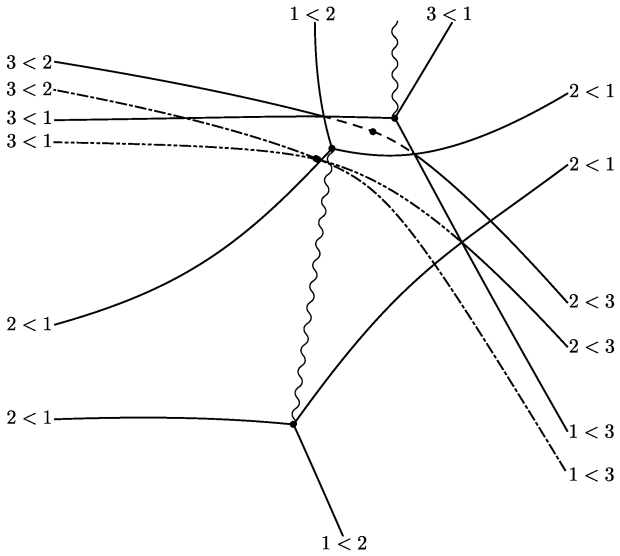

Figure 22. The Stokes geometry of the AKT_c equation for $c = c_{13}$.

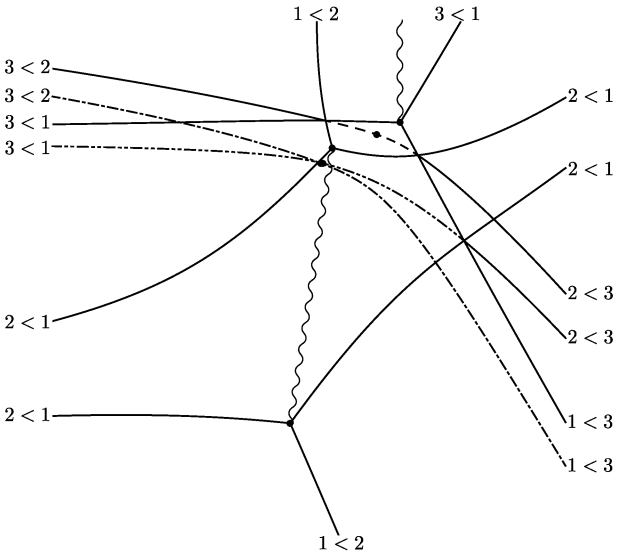

Figure 23. The Stokes geometry of the AKT_c equation for $c = c_{14}$.

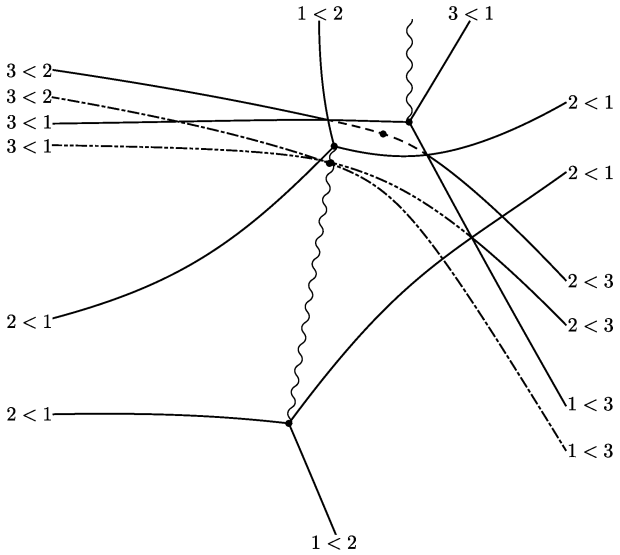

Figure 24. The Stokes geometry of the AKT_c equation for $c = c_{15}$.

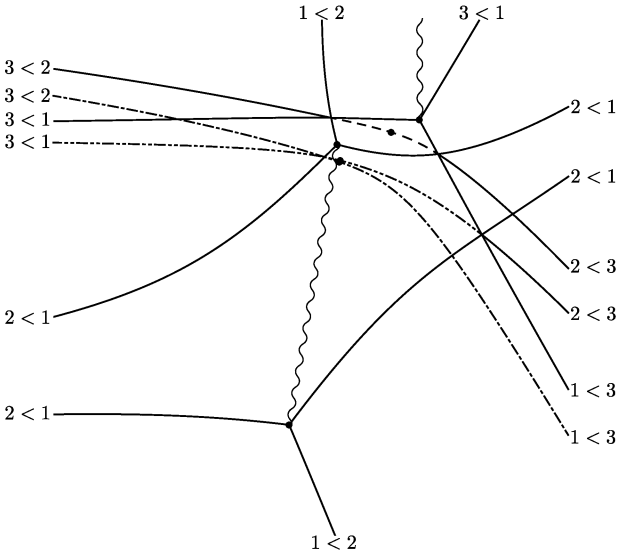

Figure 25. The Stokes geometry of the AKT_c equation for $c = c_{16}$.

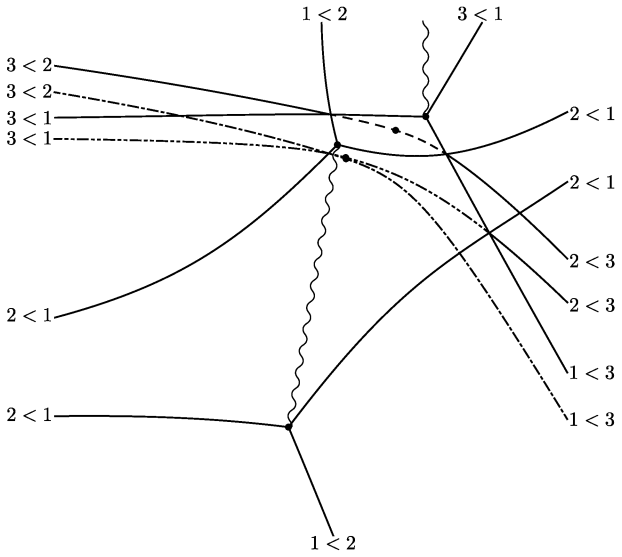

Figure 26. The Stokes geometry of the AKT_c equation for $c = c_{17}$.

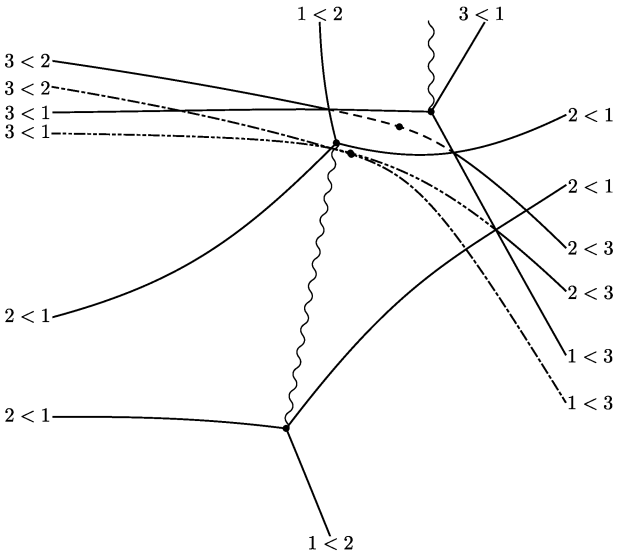

Figure 27. The Stokes geometry of the AKT_c equation for $c = c_{18}$.

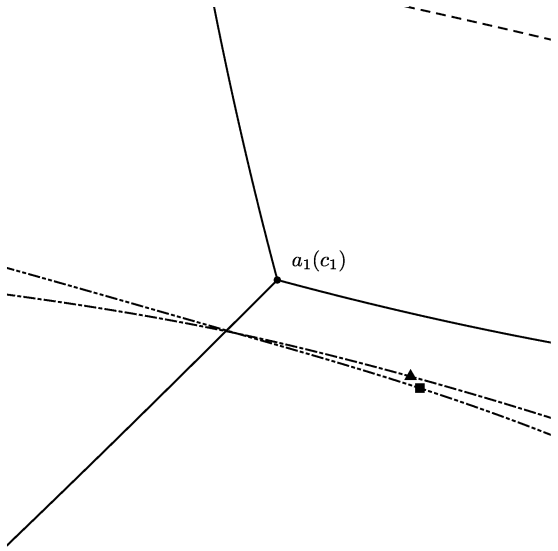

Figure 28. The enlarged version of Figure 10 around $x_1 = a_1(c_1)$. (A triangle (resp., square) designates the virtual turning point v_1 (resp., v_2).)

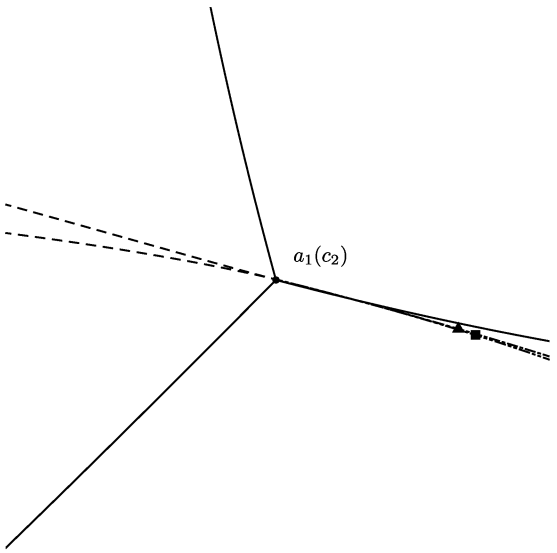

Figure 29. The enlarged version of Figure 11 around $x_1 = a_1(c_2)$. (A triangle (resp., square) designates the virtual turning point v_1 (resp., v_2).)

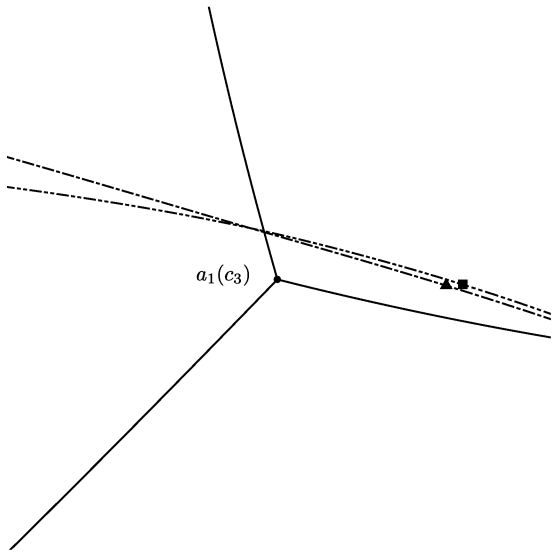

Figure 30. The enlarged version of Figure 12 around $x_1 = a_1(c_3)$. (A triangle (resp., square) designates the virtual turning point v_1 (resp., v_2).)

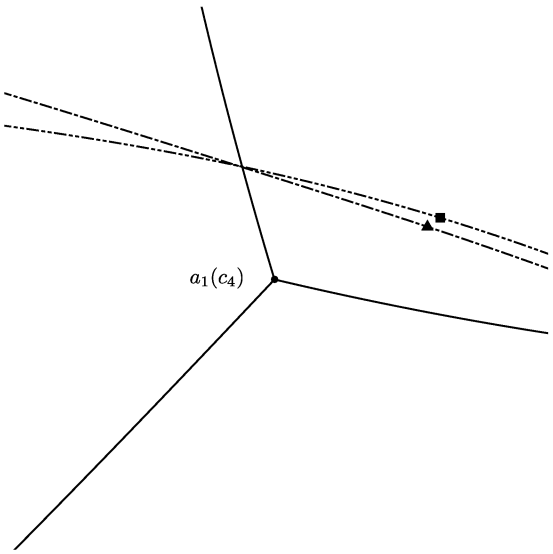

Figure 31. The enlarged version of Figure 13 around $x_1 = a_1(c_4)$. (A triangle (resp., square) designates the virtual turning point v_1 (resp., v_2).)

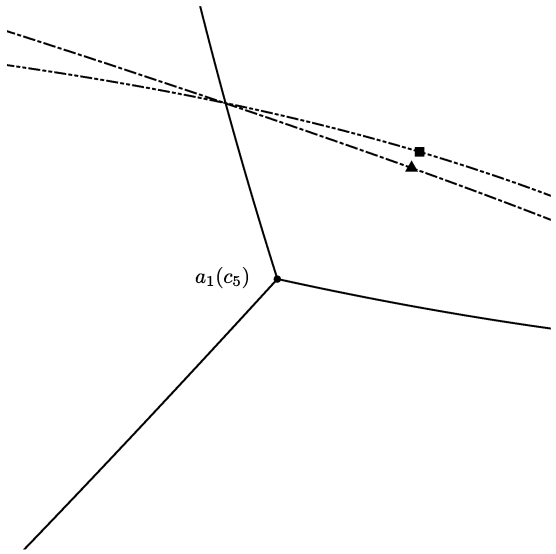

Figure 32. The enlarged version of Figure 14 around $x_1 = a_1(c_5)$. (A triangle (resp., square) designates the virtual turning point v_1 (resp., v_2).)

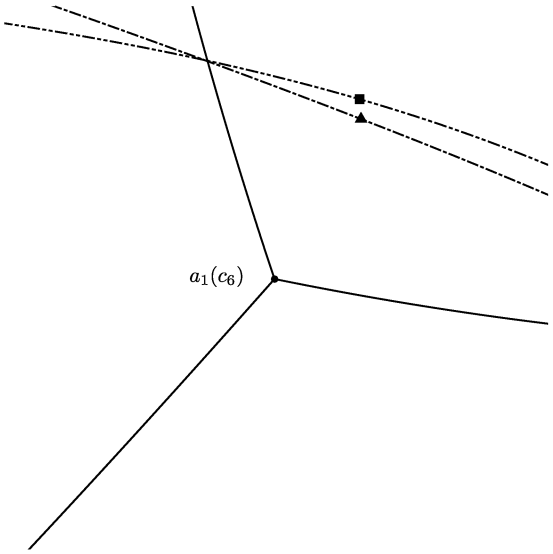

Figure 33. The enlarged version of Figure 15 around $x_1 = a_1(c_6)$. (A triangle (resp., square) designates the virtual turning point v_1 (resp., v_2).)

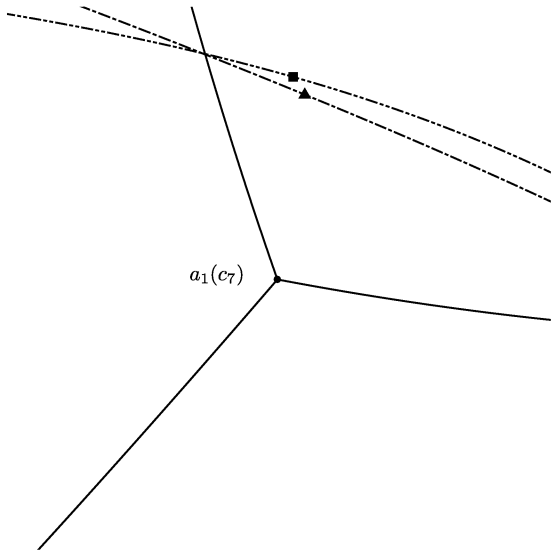

Figure 34. The enlarged version of Figure 16 around $x_1 = a_1(c_7)$. (A triangle (resp., square) designates the virtual turning point v_1 (resp., v_2).)

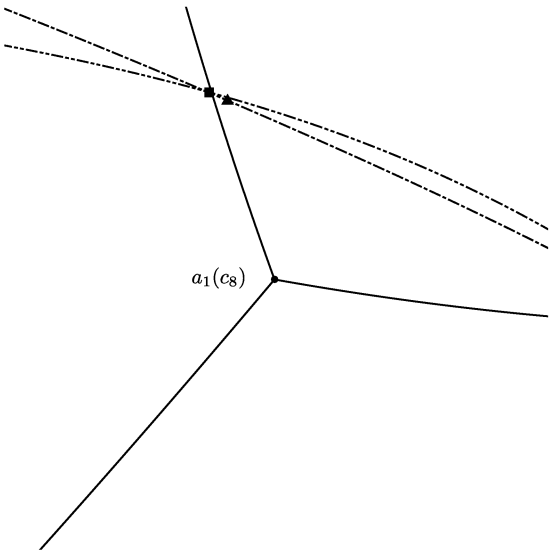

Figure 35. The enlarged version of Figure 17 around $x_1 = a_1(c_8)$. (A triangle (resp., square) designates the virtual turning point v_1 (resp., v_2).)

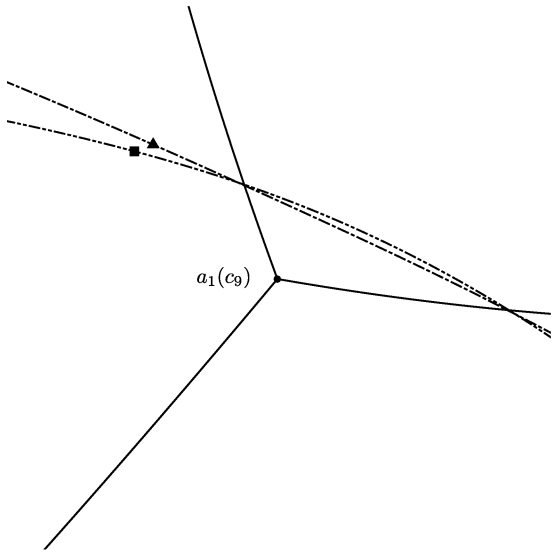

Figure 36. The enlarged version of Figure 18 around $x_1 = a_1(c_9)$. (A triangle (resp., square) designates the virtual turning point v_1 (resp., v_2).)

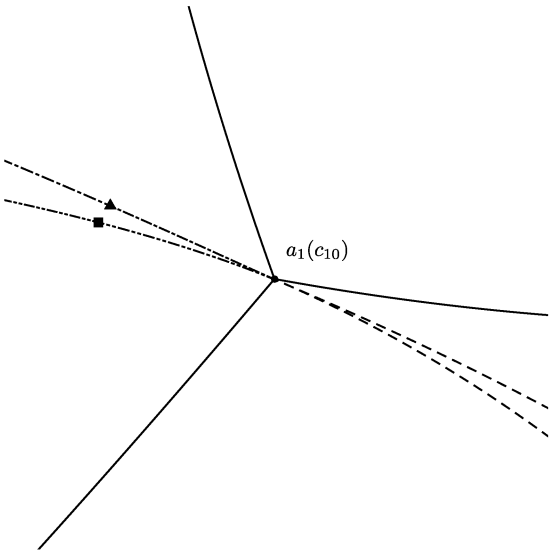

Figure 37. The enlarged version of Figure 19 around $x_1 = a_1(c_{10})$. (A triangle (resp., square) designates the virtual turning point v_1 (resp., v_2).)

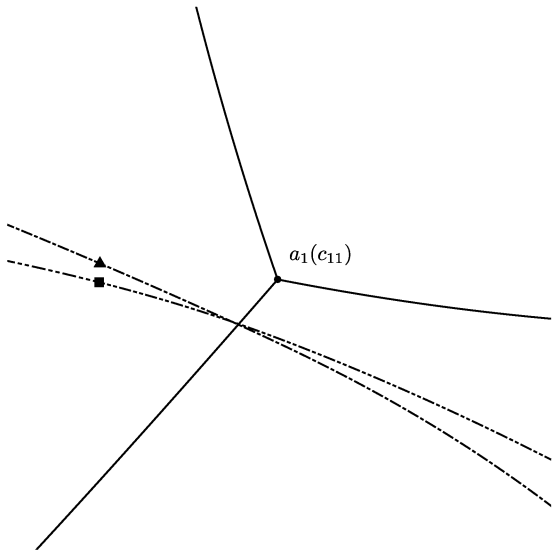

Figure 38. The enlarged version of Figure 20 around $x_1 = a_1(c_{11})$. (A triangle (resp., square) designates the virtual turning point v_1 (resp., v_2).)

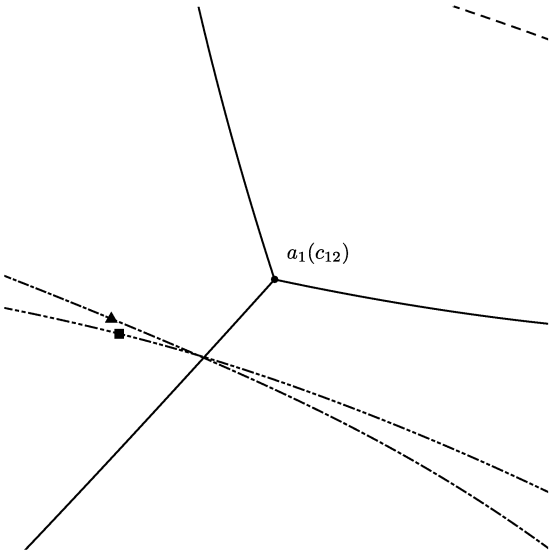

Figure 39. The enlarged version of Figure 21 around $x_1 = a_1(c_{12})$. (A triangle (resp., square) designates the virtual turning point v_1 (resp., v_2).)

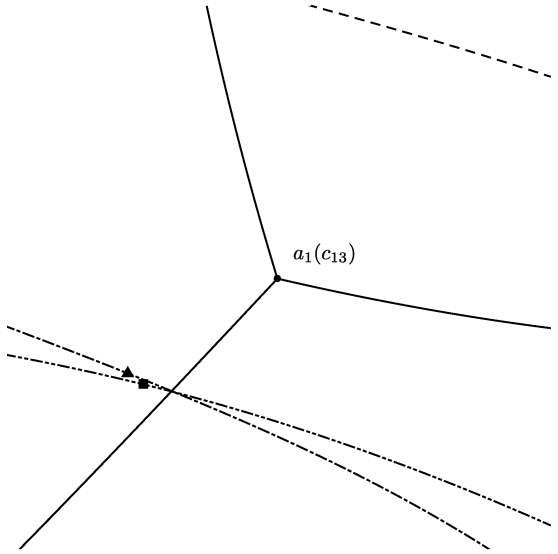

Figure 40. The enlarged version of Figure 22 around $x_1 = a_1(c_{13})$. (A triangle (resp., square) designates the virtual turning point v_1 (resp., v_2).)

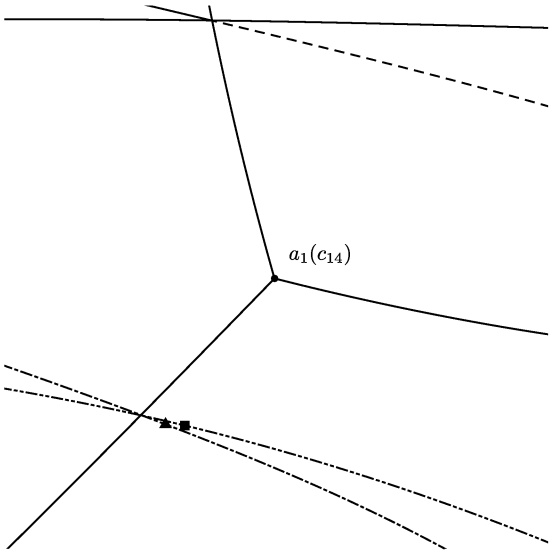

Figure 41. The enlarged version of Figure 23 around $x_1 = a_1(c_{14})$. (A triangle (resp., square) designates the virtual turning point v_1 (resp., v_2).)

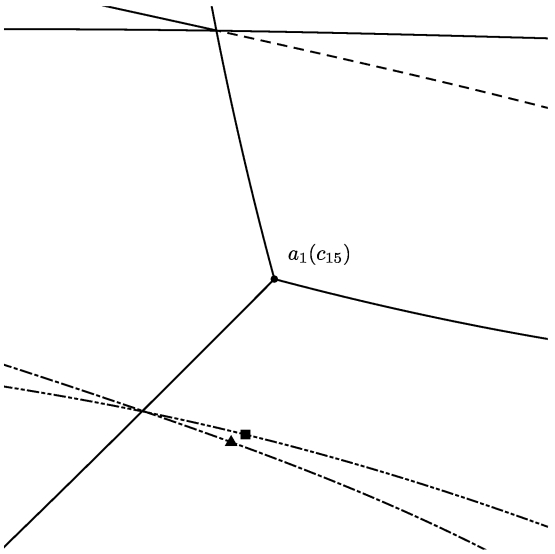

Figure 42. The enlarged version of Figure 24 around $x_1 = a_1(c_{15})$. (A triangle (resp., square) designates the virtual turning point v_1 (resp., v_2).)

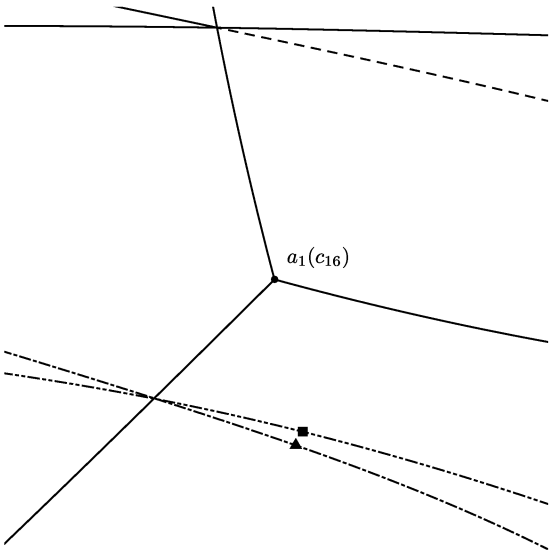

Figure 43. The enlarged version of Figure 25 around $x_1 = a_1(c_{16})$. (A triangle (resp., square) designates the virtual turning point v_1 (resp., v_2).)

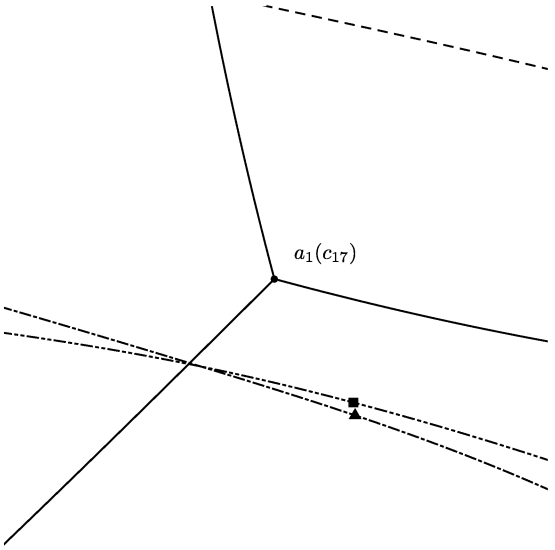

Figure 44. The enlarged version of Figure 26 around $x_1 = a_1(c_{17})$. (A triangle (resp., square) designates the virtual turning point v_1 (resp., v_2).)

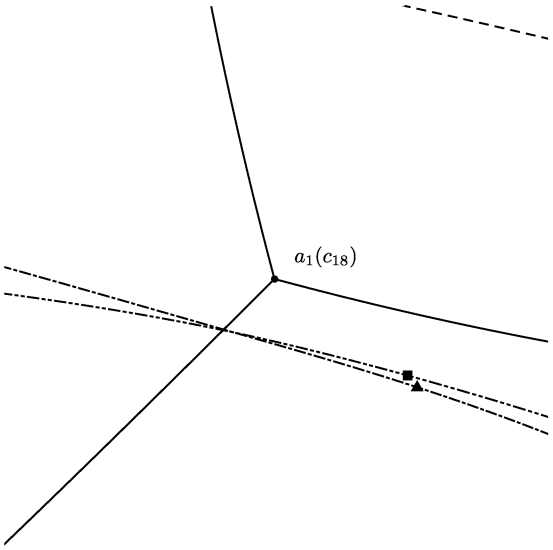

Figure 45. The enlarged version of Figure 27 around $x_1 = a_1(c_{18})$. (A triangle (resp., square) designates the virtual turning point v_1 (resp., v_2).)

points. Figures 46, 47, 48 show the Stokes geometry for $c = c_{2-\varepsilon}, c_2, c_{2+\varepsilon}$, respectively. Similarly, $c_{10-\varepsilon}$ (resp., $c_{10+\varepsilon}$) denotes the point just before (resp., shortly after) c reaches c_{10} and Figures 49, 50, 51 show the Stokes geometry for $c = c_{10-\varepsilon}, c_{10}, c_{10+\varepsilon}$, respectively. As one can readily observe in these figures, at $c = c_{10}$, where a redundant virtual turning point is changed to a non-redundant one, the new Stokes curves emanating from v_1 and v_2 simultaneously hit the ordinary turning point $a_1(c_{10})$ and it can not be determined from which virtual turning points v_1 and v_2 their portions after passing over $a_1(c_{10})$, i.e., the portions on the right side of $a_1(c_{10})$, emanate. (Having this fact in mind, we designate these portions in question by dotted line, not by chain line or two-dot chain line, in Figure 50 as well as in Figures 11, 19, 29, 37, 47.) In particular, it is impossible to determine from which virtual turning points an active portion of the new Stokes curve in question emanates. On the other hand, at $c = c_2$, similarly to the point $c = c_{10}$, the new Stokes curves emanating from v_1 and v_2 simultaneously hit the ordinary turning point $a_1(c_2)$ and it can not be determined from which virtual turning points v_1 and v_2 their portions after passing over $a_1(c_2)$ emanate. In this case, however, the portions after passing over $a_1(c_2)$ are those on the left side of $a_1(c_2)$ and hence these portions are all inert and irrelevant to the determination of the redundancy of the virtual turning points v_1 and v_2. This is the reason why a change from a non-redundant virtual turning point to a redundant one does not occur at $c = c_2$.

Summing up, a change from a non-redundant virtual turning point to a redundant one occurs only on one side of the curve (3.2.k) for $k = 1$ containing $c = c_{10}$. We also note that at a zero $c^{(1)}$ inside the closed loop γ a redundant virtual turning point and non-redundant one merge with the ordinary turning point $a_1(c)$.

We next consider the Stokes geometry of the AKT_c equation for a point c on the curve (3.2.k) for $k = 2$. It is also observed that two new Stokes curves emanating from two virtual turning points simultaneously hit an ordinary turning point on this curve. However, these two virtual turning points are both redundant and a change from a non-redundant virtual turning point to a redundant one does not occur on the curve (3.2.k) for $k = 2$. For example, we take a point $\widetilde{c}$ on the curve (3.2.k) for $k = 2$ as shown in Figure 52. Figure 53 shows the Stokes geometry of the AKT_c equation for $c = \widetilde{c}$. In Figure 53 two new Stokes curves simultaneously hit an ordinary turning point, but they are both inert. We also note that at a zero $c^{(2)}$ of (3.1.k) for $k = 2$ two virtual turning points merge with an ordinary turning point, but both of them are redundant.

More generally, we can observe with the help of a computer that, as in the case of $k = 2$, two virtual turning points merge with an ordinary turning point at a zero $c^{(k)}$ of (3.1.k) for $k \geq 3$ and new Stokes curves emanating from them simultaneously hit the ordinary turning point on the curve (3.2.k) for $k \geq 3$, but these two virtual turning points are redundant. The situations are the same also for the other curves defined by

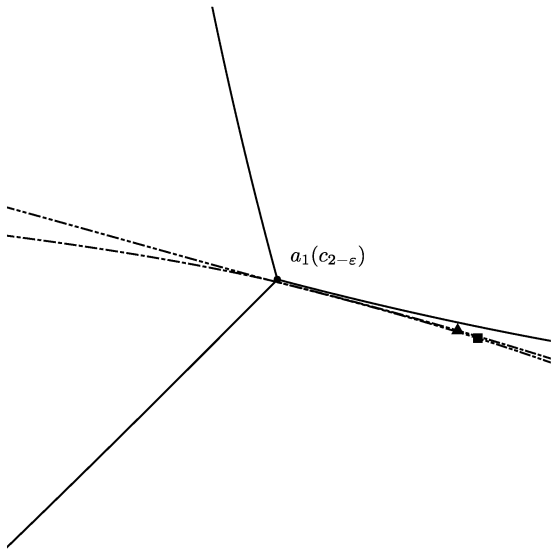

Figure 46. The Stokes geometry of the AKT_c equation around the turning point $x_1 = a_1(c)$ for $c = c_{2-\varepsilon}$. (A triangle (resp., square) designates the virtual turning point v_1 (resp., v_2).)

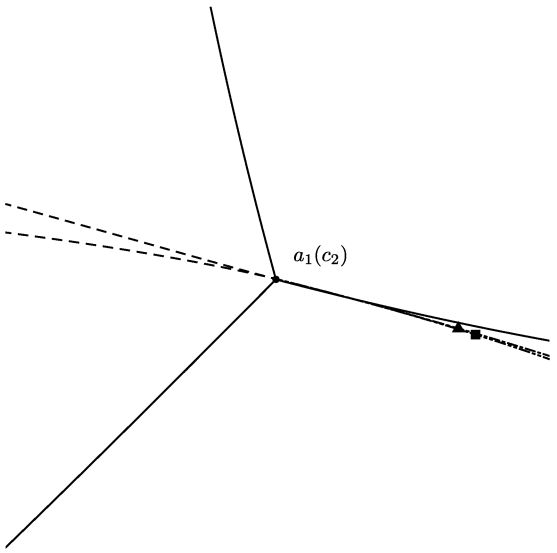

Figure 47. The Stokes geometry of the AKT_c equation around the turning point $x_1 = a_1(c)$ for $c = c_2$. (A triangle (resp., square) designates the virtual turning point v_1 (resp., v_2).)

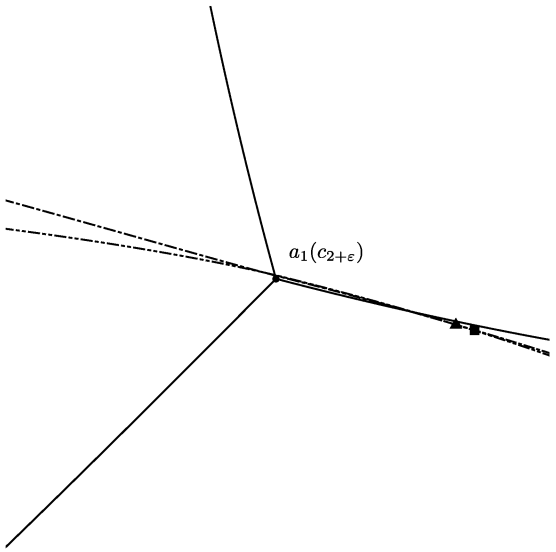

Figure 48. The Stokes geometry of the AKT_c equation around the turning point $x_1 = a_1(c)$ for $c = c_{2+\varepsilon}$. (A triangle (resp., square) designates the virtual turning point v_1 (resp., v_2).)

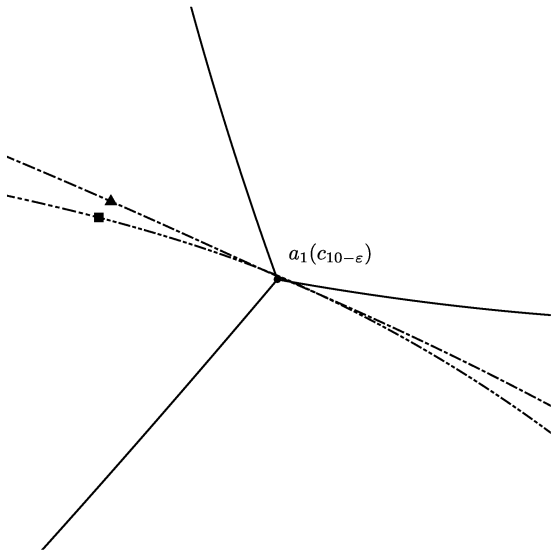

Figure 49. The Stokes geometry of the AKT_c equation around the turning point $x_1 = a_1(c)$ for $c = c_{10-\varepsilon}$. (A triangle (resp., square) designates the virtual turning point v_1 (resp., v_2).)

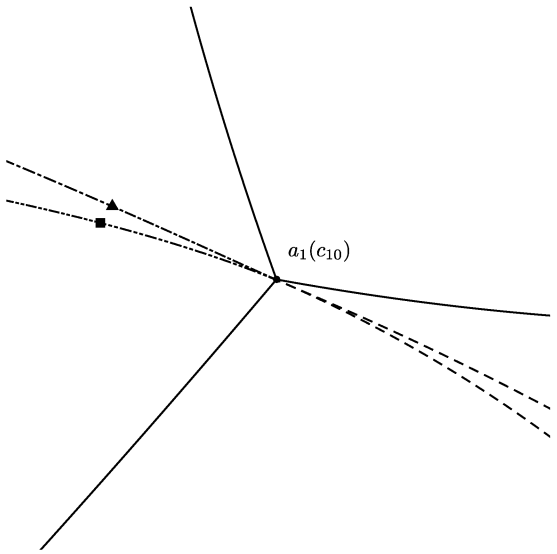

Figure 50. The Stokes geometry of the AKT_c equation around the turning point $x_1 = a_1(c)$ for $c = c_{10}$. (A triangle (resp., square) designates the virtual turning point v_1 (resp., v_2).)

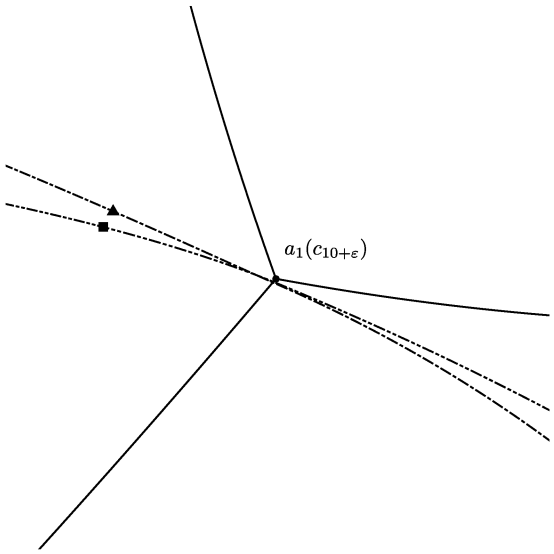

Figure 51. The Stokes geometry of the AKT_c equation around the turning point $x_1 = a_1(c)$ for $c = c_{10+\varepsilon}$. (A triangle (resp., square) designates the virtual turning point v_1 (resp., v_2).)

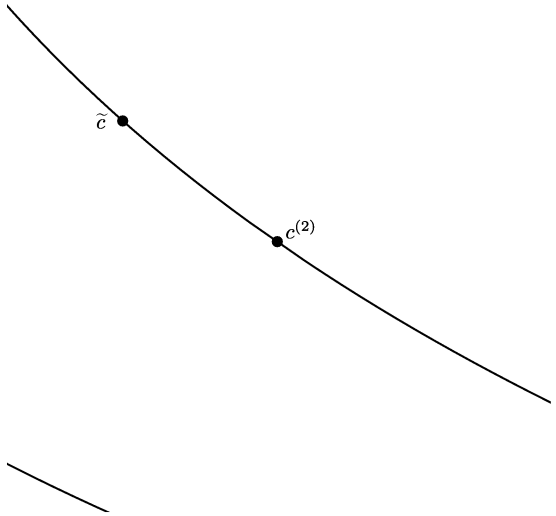

Figure 52. $c^{(2)}$ and $\widetilde{c}$.

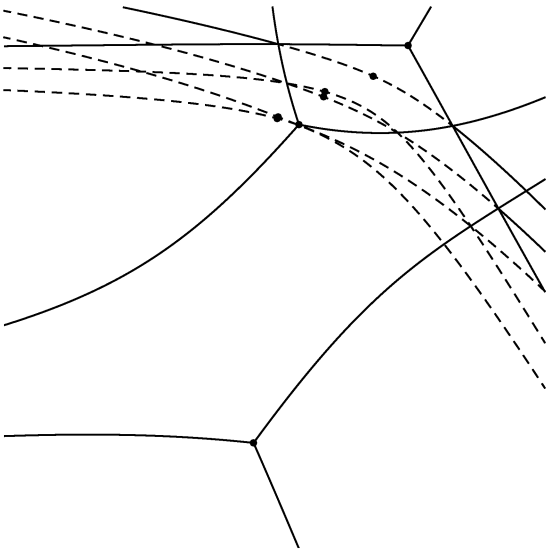

Figure 53. The Stokes geometry of the AKT_c equation for $c = \widetilde{c}$.

(3.2.k).

§ 4. Concluding remark

Summing up what we have observed in §3, we obtain Figure 54. In Figure 54 we draw only the curves (2.2) for $k = \pm 1, \ldots, \pm 6$ and use solid (resp., dotted) line to designate a portion of the curves where a change from a redundant virtual turning point to a non-redundant one is observed (resp., is not observed). As clearly shown in Figure 54, such a change is observed only on three curvilinear half lines, although the number of the curves (2.2) is infinite. Thus it turns out that a redundant virtual turning point of the AKT_c equation may become a non-redundant one when the parameter c changes and that such a change occurs along a curvilinear half line explicitly defined by the relation (2.2). We expect that this intriguing observation plays an important role in introducing a proper definition of the redundancy of virtual turning points for a general higher order equation depending on parameters in our future study.

Furthermore, in the case of the AKT equation the number of non-redundant virtual turning points is finite. Note that Honda [3] discusses the finiteness of the number of non-redundant virtual turning points for a general higher order equation by using a completely different argument based on his "depth functions". In this paper we confirmed such finiteness for the AKT_c equation by studying its deformation with respect to the parameter c. As emphasized in [2], study of the deformation of the AKT_c equation with respect to c is closely related to considering the extended holonomic system, i.e., the

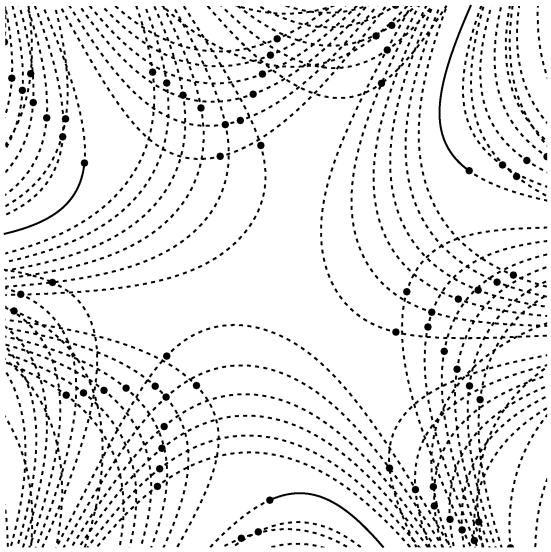

Figure 54. The curves (2.2) for $k = \pm 1, \ldots, \pm 6$. Here portions where a change from a redundant virtual turning point to a non-redundant one is observed (resp., is not observed) are drawn by solid (resp., dotted) line.

(1,4) hypergeometric system. To discuss the finiteness of the number of non-redundant virtual turning points for more general higher order equations in conjunction with the study of their extended holonomic systems is also an important future problem.

References

[1] T. Aoki, T. Kawai and Y. Takei, New turning points in the exact WKB analysis for higher order ordinary differential equations, *Analyse algébrique des perturbations singulières, I, Méthodes résurgentes*, Hermann, 1994, pp. 69-84.

[2] S. Hirose, On the Stokes geometry for the Pearcey system and the (1,4) hypergeometric system, *RIMS Kôkyûroku Bessatsu*, B40 (2013), 243-292.

[3] N. Honda, The geometric structure of a virtual turning point and the model of the Stokes geometry, *RIMS Kôkyûroku Bessatsu*, B10 (2008), 63-113.

[4] N. Honda, T. Kawai and Y. Takei, Virtual Turning Points, SpringerBriefs in Mathematical Physics, Vol. 4, Springer-Verlag, 2015.